

CORRECTED

WIND EROSION MECHANICS: ABRASION OF AGGREGATED SOIL

L. J. Hagen
ASSOC. MEMBER
ASAE

ABSTRACT

The wind erosion process on agricultural soils is being modeled as the time-dependent conservation of mass transport of soil moving as saltation and creep. Emission of loose soil and abrasion of clods and crust act as sources, whereas trapping and suspension act as sinks for the moving soil. In this study, an expression for the abrasion source term was derived. Abrasion flux from aggregates or crust was shown to be the product of three variables – fraction of saltation impacting the target, an abrasion coefficient, and saltation discharge. Various aspects of the proposed abrasion source term were then investigated in three wind tunnel studies. First, crusted trays were abraded using a range of windspeeds and sand abrader rates. Regression analysis showed there was no significant relationship between crust abrasion coefficients and fraction of abrader moving below 0.1 m (i.e. abrader trajectories). This result shows practical abrasion coefficients can be developed which depend only on the properties of the target and abrader. Second, a relationship was developed to predict fraction of saltation impacting surface aggregates (or intervening crust) as a function of surface aggregate cover and roughness. The relationship was tested in the tunnel by abrading crusted trays partially covered (0 to 30%) with non-abradable aggregates. Regression analysis showed there was good agreement ($R^2 = 0.97$) between observed and predicted fraction of abrader impacting aggregates. In the third experiment, trays were filled with various mixtures of large- and saltation-size aggregates. The trays were abraded in the wind tunnel by a low saltation discharge from a narrow upwind aggregate bed. The results showed that, because the wind transport capacity significantly exceeded the saltation discharge, the surface tended to armor with large aggregates. In this case, the fraction of abrader impacting large aggregates was not significantly different from one for a wide range of aggregate mixtures.

KEYWORDS. Wind, Erosion, Modeling.

INTRODUCTION

The United States Department of Agriculture has initiated a major effort to develop technology to replace the current wind erosion equation (Woodruff and Siddoway, 1965) with a computer model that simulates erosion, as well as the weather, hydrology, soil, tillage, and biomass conditions that control wind erosion (Hagen, 1988). The new model has a modular structure that will include a number of different submodels.

Wind erosion on agricultural soils is not a single process, rather, it consists of a series of subprocesses, which are partially dependent on one another (Hagen, 1990). Thus, to simulate wind erosion, the important subprocesses that control the mass conservation of eroding soil in the saltation and creep transport modes must be modeled. These processes are emission of the loose soil aggregates by wind and impact of saltating aggregates, trapping (deposition) of saltation and creep, suspension of fine particles created by emission or abrasion, and finally, the abrasive breakdown of aggregates or crust to wind-erodible size. This study was concerned mainly with the latter process.

Chepil and Woodruff (1963) discussed formation of the various soil structural units and listed their relative mechanical stability in the dry state from highest to lowest as follows: (a) water-stable aggregates, (b) secondary aggregates or clods, (c) surface crust, and (d) fine materials among the clods. Because the water-stable aggregates are generally less than 1.0 mm in diameter, only the other structural units are capable of providing a stable surface cover. The stability of aggregates less than 1.0 mm in diameter is important, however, because they serve both as abraders and as a major source of suspended soil (Hagen and Lyles, 1985).

Using a calibrated sand-blasting nozzle in a test chamber, the abrasion loss from individual soil aggregates has been investigated (Hagen, 1984; Hagen et al., 1988). In general, the abrasion loss increased with decreasing impact angles and increasing abrader diameter. Using sand as the abrader increased abrasion loss about 10% above the loss caused by using soil aggregates as the abrader. Wetting the target aggregates usually caused their abrasion rate to decrease. However, by far the most important variables were the kinetic energy (i.e., mass times velocity squared) of the impacting abrader and the dry aggregate stability of the target aggregates. The latter variable was measured by a drop-shatter test and more recently by an aggregate crushing energy test (Skidmore and Powers, 1982).

It seems likely that aggregates at an eroding field surface will respond to saltation impacts in a similar manner. However, the process at the field surface is more

Article was submitted for publication in November 1990; reviewed and approved for publication by the Soil and Water Div. of ASAE in March 1991. Presented as ASAE Paper No. 88-2561.

Contribution from the USDA-ARS, in cooperation with Department of Agronomy, Kansas Agricultural Experiment Station. Contribution No. 91-205J.

The author is Lawrence J. Hagen, Research Leader, USDA-ARS, Kansas State University, Manhattan.



complex than in the test chamber because the saltating particles impact a given surface area with a wide range of velocities and impact angles. Hence, the objective of this study was to develop methodology useful to predict the abrasion rate of an aggregated soil surface for the EROSION Submodel of the new Wind Erosion Research Model.

THEORY

On agricultural soils, the erosion process can be modeled as the time-dependent conservation of mass of two species (saltation and creep size aggregates) with two sources of erodible material (emission and abrasion) and two sinks (surface trapping and suspension). A computational control volume using this scheme for a bare soil is illustrated in figure 1. The equations for mass conservation of saltating aggregates on a two-dimensional rectangular field can be written as:

$$\frac{\partial \bar{C}H}{\partial t} = -\frac{\partial q_x}{\partial x} - \frac{\partial q_y}{\partial y} + G_{en} + G_{an} - G_{tp} - G_{ss} \quad (1)$$

$$q = (\bar{C}H) \bar{V}_p \quad (2)$$

$$\bar{V}_p = K_p U_* \quad (3)$$

$$q_x = (EU/WU) q \quad (4)$$

$$q_y = (EV/WU) q \quad (5)$$

where

x and y = horizontal distances in perpendicular directions parallel to the field boundaries;

t = time;

\bar{C} = average concentration of saltating particles in the control volume of height H ;

q_x and q_y = components of the saltation discharge, q , in the x and y directions, respectively;

\bar{V}_p = average horizontal saltation particle velocity;

K_p = a proportionality coefficient;

U_* = surface friction velocity;

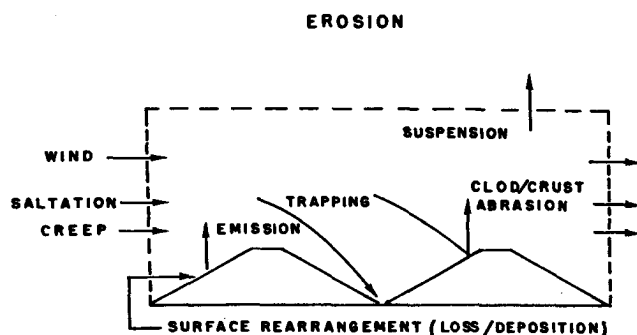


Figure 1—Diagram of a control volume for the EROSION submodel with bare soil.

EU and EV = components of the horizontal wind speed, WU , in the x and y directions, respectively; and

G_{en} , G_{an} , G_{tp} , and G_{ss} represent net vertical soil fluxes from emission of loose soil, surface abrasion of aggregates/crusts, trapping of saltation, and suspension of fine particles, respectively.

A similar set of equations can be written for mass conservation of the creep component. Finally, auxiliary equations to describe the changes in the soil surface in response to loss or deposition are needed to complete the system of equations.

To solve the system of equations, expressions must be derived for the source-sink terms, such as G_{an} . The cited chamber studies demonstrated that abrasion loss was proportional to the kinetic energy of the impacting abrader per unit area. Thus, an approximation for G_{an} is:

$$G_{an} = C_1 \sum_{i=1}^n G_i V_i^2 \quad (6)$$

where

C_1 = a coefficient that depends on the properties of the abrader and target aggregates or crust,

G_i = the mass flux of impacting particles that follow the i th trajectory, and

V_i = their average impact velocity. Now,

$$G_i = (q_i / L_i) \quad (7)$$

where

q_i = the horizontal discharge of particles (with units $ML^{-1}T^{-1}$) that follow the i th saltation trajectory, and

L_i = their average particle jump length.

Schematic saltation trajectories for two groups of particles are illustrated in figure 2. At impact, the average impact angle, θ_i , for the i th group is:

$$\theta_i = \tan^{-1} (-w_i / u_i) \quad (8)$$

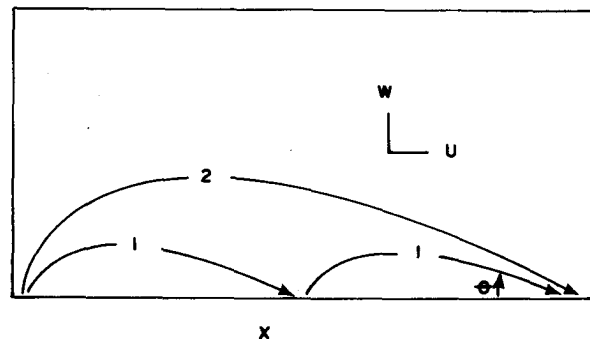


Figure 2—Average saltation trajectories for two groups of particles with vertical velocities, w ; horizontal velocities, u ; impact angles, θ ; and impact velocities, V_i .

where w is the vertical component, and u is the horizontal component of abraders velocity. The ratio of impact velocities, V_i , can be written as:

$$\frac{V_2}{V_1} = \frac{w_2 \left(\frac{1}{\tan^2(\theta_2)} + 1 \right)^{1/2}}{w_1 \left(\frac{1}{\tan^2(\theta_1)} + 1 \right)^{1/2}} \quad (9)$$

and, neglecting differences in the vertical air drag on the two groups, the ratio of vertical velocities at impact is:

$$\frac{w_2}{w_1} = \left[\frac{2gz_2}{2gz_1} \right]^{1/2} \quad (10)$$

where

g = acceleration of gravity, and
 z = maximum particle jump height.

Both particle diameter and lift-off velocity affect the flight path of individual particles. Nevertheless, calculations of impact angles show that they are only weakly dependent on lift-off velocity (Anderson and Hallet, 1986). Further, White (1982) reported that the logarithm of saltation flux decreased linearly with height, regardless of wind speed, particle size, and ambient pressure.

The preceding evidence suggests that average trajectories for two groups of particles are similar. Thus, $\theta_1 = \theta_2$, and $z_2/z_1 = L_2/L_1$, where L is average horizontal jump distance traveled in a single bound. Because V_2 and V_1 are chosen arbitrarily, it follows that:

$$V_i^2/L_i = \text{constant} \quad (11)$$

and

$$G_{an} = C_{an} q \quad (12)$$

where $C_{an} = C_1(V_i^2/L_i)$ and $\Sigma q_i = q$. C_{an} is a proportionality constant dubbed coefficient of abrasion with units $1/L$. C_{an} should be largely independent of both the wind speed and magnitude of q , but should vary with the properties of the target surfaces and the abraders. The dominant independent predictor variable is the target dry aggregate stability, as found in the chamber studies.

When the abraded soil surface is complex, the incoming saltation may strike large aggregates, crust, or other saltation-size particles. To account for the different impact surfaces, equation 12 can be modified to:

$$G_{an} = \left(\sum_{i=1}^n F_{ani} C_{ani} \right) q \quad (13)$$

where F_{ani} is the fraction of q impacting the i th surface, which has a coefficient of abrasion, C_{ani} . It will be assumed

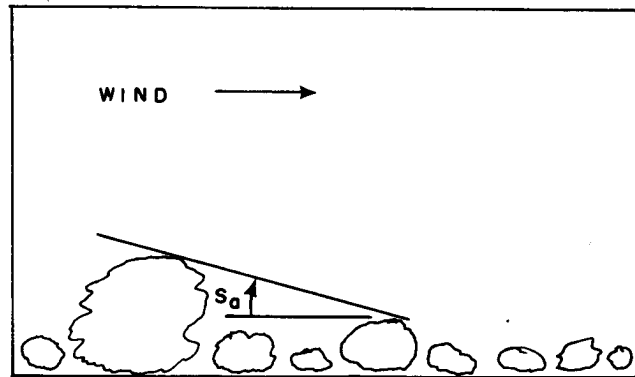


Figure 3—Diagram illustrating shelter angle, S_a , at a single point as the largest angle above horizontal that intersects the upwind soil surface.

that incoming q above the surface is uniformly distributed. For impact surfaces of residue, rock, and aggregates less than creep-size, C_{ani} is zero.

For an aggregated surface, F_{ani} for large aggregates depends on the surface roughness, as well as the fraction of surface covered with large aggregates, F_{sc} . To analyze the effect of surface roughness, the roughness can be described as a distribution of shelter angles (S_a) as defined at a single point in figure 3. From transects of surface height measurements, S_a can be calculated for each point, and the Weibull distribution used to represent this measure of field surface roughness (Potter et al., 1990). The cumulative distribution has the form:

$$F(S_a) = 1 - \exp\left(-\left(\frac{S_a}{RR1}\right)^{RR2}\right) \quad (14)$$

where $RR1$ (degrees) is the scale factor and related to average shelter angle as:

$$\bar{S}_a = RR1/1.12, \quad (15)$$

and $RR2$ is the shape factor, which ranges from about 1 to 2 for soils. If we assume that: a) the large aggregates are the cause of the sheltered zones; and b) on average, the zones sheltered from impacts have shelter angles $>12^\circ$, F_{ani} for large aggregates can be calculated as:

$$F_{ani} = F_{sc} + F_{>12} = F_{sc} + \exp\left[-\left(\frac{12}{RR1}\right)^{RR2}\right]; \quad (16)$$

$$0 \leq F_{ani} \leq 1$$

where $F_{>12}$ is the fraction of surface with shelter angles $>12^\circ$. A 12° average saltation impact angle was selected because it is within the range commonly measured by other researchers (Willettts and Rice, 1985). Equation 16 represents an upper bound on F_{ani} because a part of F_{sc} could occur in the sheltered zone. However, most eroding surfaces have 30% or more saltation-size aggregate cover, which will occupy the sheltered zone. The theories

proposed in equations 12 and 16 are simplifications of a complex process, so two experiments were undertaken to test critical assumptions in their derivations.

Although F_{ani} is dynamic and can range from 0 to 1 on a given field, there are a range of conditions for which F_{ani} probably can be defined. These conditions occur when the wind saltation transport capacity far exceeds q over the aggregated surface. In these areas, the exposed, saltation-size particles should be quickly removed or remain only in areas sheltered from impact, and F_{ani} for the large aggregates should be near 1. Further, the rate of soil loss should be controlled by the rate of abrasion of the large aggregates, which provide the surface armor. Thus, $F_{ani}C_{ani}$ should be nearly constant, regardless of the proportions of large and saltation-size aggregates in the soil mixture. To test this hypothesis, a third wind tunnel experiment was undertaken.

EXPERIMENTAL PROCEDURE

FIRST EXPERIMENT

The first experiment was designed to test the hypotheses in equation 12 that mean saltation trajectories had little effect on C_{an} . Trays with an area of 0.51 m² and depth of 5 cm were filled with sieved soil smaller than 2 mm in diameter. The trays were wetted from the bottom by capillary action and air-dried. Shrinkage cracks were then filled with additional soil, wetted, and again air-dried. This procedure produced a weakly consolidated but homogenous soil mass in each tray. The soils selected were a Wymore silty clay loam (Aquic Argiduoll) and a Reading silt loam (Typic Argiduoll).

Abrasion tests on the trays were conducted as follows. Each tray was centered near the downwind end of a wind tunnel with a 1.52 x 1.82 x 15.3 m working section. The tray top surface was positioned parallel with a floor composed of 2 to 6 mm diameter gravel. Beds of various lengths filled with 0.29 to 0.42 mm diameter quartz sand were placed 50 mm deep across the upwind tunnel width, and the sand was blown across the tray for 90-s runs.

The experiment was planned as a randomized complete block design with two soils comprising the blocks and five upwind sand bed lengths (0.23 to 10.0 m) as treatments. Variations in sand bed length were used to establish various levels of median saltation trajectories. A short sand bed prevents the saltation load from reaching transport capacity, and the excess wind energy then forces the particles to jump higher than at transport capacity. Freestream wind speeds were varied between test runs and ranged from 13.5 to 15.8 m/s. There were four trays of each soil and five runs on each tray for a total of 40 test runs. After each run, loose soil was blown from the tray, and the tray was weighed to determine abraded soil loss. Soil abraded passage over the tray was measured by a pair of vertical slot samplers placed leeward of the tray. One of the samplers also was segmented to permit sampling the vertical profile of saltating material. A small amount of abraded soil was of saltation-size and collected as part of the abraded, but suspension-size, abraded soil passed through the sampler. For each run, C_{an} was calculated as the ratio of tray soil loss per unit area to abraded passage per unit width. Finally, the saltation transport capacity

(q_{max}) based on measured values with long sand beds was compared to the measured saltation transport (q) with the short sand beds.

SECOND EXPERIMENT

The second experiment was designed to test the hypothesis that F_{ani} could be calculated as proposed in equation 16. Crusted trays of Wymore soil were again prepared as described in experiment 1. Next, surface covers of 5, 10, 20, and 30% of simulated, non-abradable aggregates (buildex rock) were placed at random on the trays; some trays had no cover. Two different sizes of sieved rock were used for tray cover, 6.4 to 12.8 or 25.4 to 38.1 mm diameter.

Similar to experiment 1, the trays were abraded in the wind tunnel, and the reduction in abrasion loss from the crust on trays with cover compared to no cover was interpreted as a measured value of F_{ani} , i.e., the fraction of abraded impacting on the rock cover. Next, a pin meter (10 mm pin spacing) was used to measure roughness of the trays with cover. The Weibull distribution (equation 14) was fitted to the roughness heights, and the roughness parameters RRI and RR2 were calculated. Predicted values of F_{ani} for each surface cover were then calculated using equation 16.

THIRD EXPERIMENT

When q_{max} substantially exceeds q , $F_{ani}C_{ani}$ should be nearly constant on a uniform aggregate bed. Equations were developed to calculate $F_{ani}C_{ani}$ for large aggregates, using total soil loss from a wind tunnel test tray containing only large aggregates and saltation-size soil. Based on mass conservation, total soil loss per unit area, (TL), can be described as:

$$TL = E_0 + (G_{enz} + F_{ani} C_{ani} q) t \quad (17)$$

where E_0 is the initial saltation-size soil removable by wind alone, G_{enz} is the saltation-size soil emitted from the surface as it is uncovered by abrasion during time, t , and the last term is the abrasion loss.

Now for a uniform mixture with depth, the emission loss and abrasion loss must be proportional to their respective volumes, V_{en} and V_{an} , such that:

$$G_{enz} / (F_{ani} C_{ani} q) = V_{en} / V_{an} \quad (18)$$

The solution then becomes:

$$F_{ani} C_{ani} = (TL - E_0) / [qt (1 + V_{en} / V_{an})] \quad (19)$$

An experiment was carried out in an outdoor wind tunnel to determine if $F_{ani}C_{ani}$ behaved as postulated.

Soil samples for testing were obtained from the Ap horizon of a Haynie (Mollic Udifluent) soil with a very fine sandy loam texture. The soil samples were sieved, and four mixtures were prepared with large aggregates (F_c) comprising 12, 33, 60, or 67% by mass. The large aggregates ranged from 6.0 to 19.1 mm sieve diameter,

whereas the small aggregates ranged from 0.15 to 0.59 mm.

Individual soil mixtures were placed in a 430 x 1720 x 30 mm tray, which was mounted on a weighing device located such that the top of the tray was parallel with the surface of the wind tunnel floor. The wind tunnel was an open ended, push-type with a 0.91 x 0.91 m cross-section and 12.2 m length. The floor of the tunnel was covered with 2 to 6 mm diameter gravel imbedded in soil particles.

During tests, loose, saltation-size soil was removed from the tray by wind alone to form an armored surface. Next, weighed amounts of soil abrader, 0.15 to 0.59 mm in diameter, were spread uniformly across the tunnel floor near the tunnel entrance and blown across the downwind test tray. By restricting the length of the abrader bed to <0.5 m, q was restricted to 30 to 60% of the wind transport capacity. After each abrasion treatment, wind alone was used to stabilize the soil surface, and the total soil loss was recorded by the weighing mechanism. Freestream wind speed was recorded during all tests. Two or three trays of each aggregate mixture were tested at 12.5 and 15.5 m/s freestream wind speeds. Finally, the distribution of abrader across the tunnel cross section was monitored by two vertical slot samplers located downwind from the tray. Abrader collected by the slot samplers was used to calculate the ratio of abrader crossing the tray compared to the total abrader moving down the tunnel.

RESULTS AND DISCUSSION

FIRST EXPERIMENT

The crusted, bare trays were easily abraded and had a mean C_{an} 0.154 ± 0.031 . The treatments did not produce statistically significant differences in C_{an} between treatments or soils (Table 1), even though there were differences in the ratio of saltation discharge (q) to saltation transport capacity (q_{max}). Since there were no apparent treatment differences between soils, the data were combined, and the percentage q trapped below 0.1 m was calculated for each run. Next, to better illustrate their range, these data were normalized by dividing by the largest value of percentage q trapped below 0.1 m. Finally, C_{an} were compared to the normalized percentage of q trapped below 0.1 m height for each run (fig. 4). Although the fraction of saltation discharge moving below 0.1 m varied by nearly a factor of 2 among test runs, the correlation to C_{an} was not significant.

TABLE 1. Average abrasion coefficients, C_{an} , of crusted trays. No significant differences (0.10 level) between treatments or soils, each replicated four times

Treatment Variables	Soils	
	Wymore Silty Clay Loam	Reading Silt Loam
$\frac{q}{q_{max}}$		
	----- m^{-1} -----	
0.35	0.16	0.19
0.71	0.15	0.16
1.00	0.14	0.14
0.99	0.15	0.14
0.99	0.18	0.15

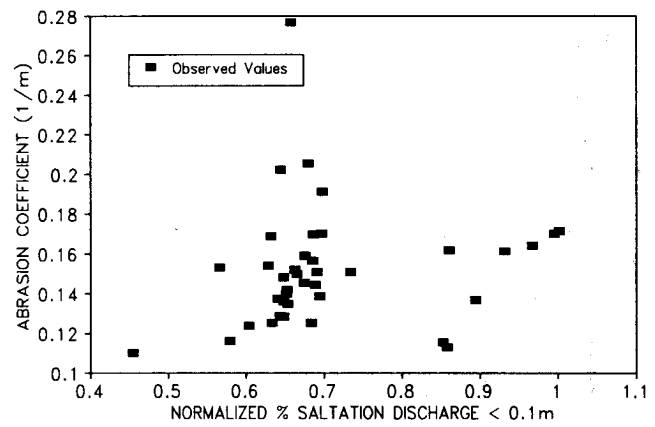


Figure 4—Abrasion coefficient (C_{an}) of crusted surfaces as a function of normalized percentage of saltation discharge below 0.1 m. Linear regression analysis showed no significant correlation.

As Sorensen (1985) has shown in detail, large changes in the vertical profiles of measured saltation discharge signify large changes in saltation particle trajectories. Thus, for practical use, C_{an} can be considered independent of saltation trajectories, as suggested in equation 12. Additional experiments might reveal a small effect of saltation trajectories on C_{an} , but dry soil stability dominates the response to abrasion. Hence, major improvements in prediction of C_{an} can come only from improved predictions of temporal dry stabilities of field aggregates and crusts.

SECOND EXPERIMENT

The predicted values of F_{ani} , using measured values of tray roughness in equation 16, are depicted by smooth, continuous lines through these points in figure 5. The measured values of F_{ani} inferred from the crust abrasion losses are shown as individual data points. In general, there was good agreement between predicted and observed values ($R^2=0.97$), when average impact angle was selected at 12° . Selecting higher or lower average impact angles in

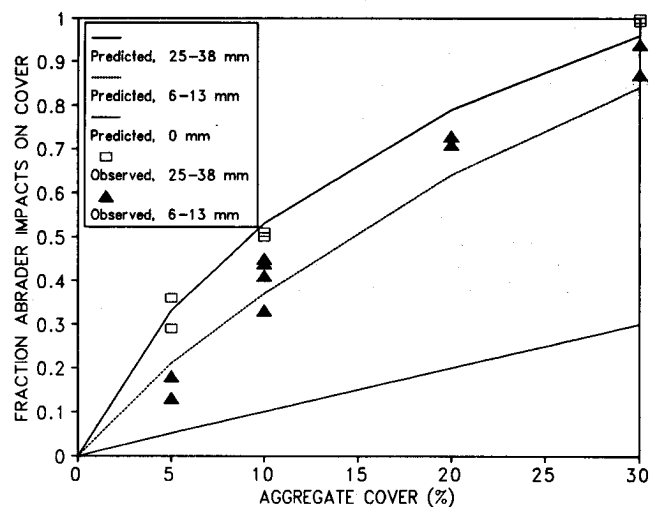


Figure 5—Comparison of fraction of saltation impacts on surface aggregates predicted using surface cover and roughness (lines) to measured fraction of surface impacts for two sizes of rock aggregate cover. Zero line is predicted impact on cover without roughness.

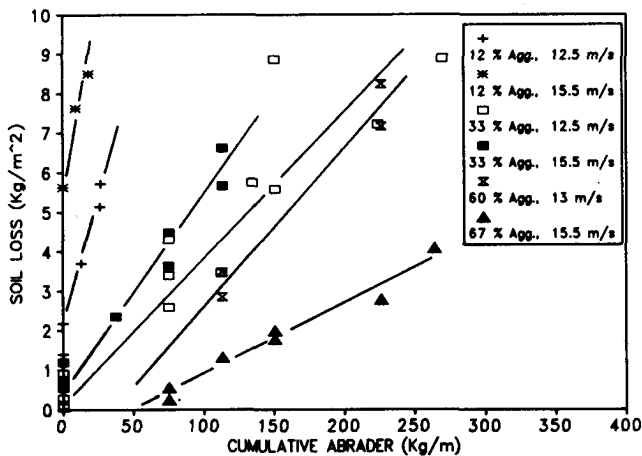


Figure 6—Cumulative soil loss from wind tunnel trays in response to cumulative amounts of abrader at various levels of large aggregate mass in the soil mixtures and freestream wind speeds.

1° steps produced lower R² values between predicted and observed. For contrast, the fraction of impacts expected for zero height cover also is shown on figure 5.

THIRD EXPERIMENT

Total soil loss from the trays was generally linearly proportional to the cumulative abrader passage, with coefficients of determination (R²) ranging from 0.89 to 0.97 (fig. 6). The intercepts at zero abrader represent the loss of saltation-size aggregates by wind alone at the beginning of each test. As the proportion of large aggregates, F_c, increased, the initial soil loss decreased. Indeed, with 60 and 67% F_c, some abrader initially may have been trapped among the aggregates at the test wind speeds.

The slope of the soil loss versus cumulative abrader lines represents the rate of total soil loss from abrasion as well as emission of saltation-size particles. The formula presented in equation 19 was used to compute F_{ani}C_{ani} for each treatment combination represented by individual data points with abrader greater than zero, and the means for each wind speed are shown in Table 2.

Analysis of variance indicated that none of the treatment means were different (0.10 level). Because all the test aggregates were selected from a single soil sample, C_{ani} should have been constant over all reps. Thus, the result shows that F_{ani} was also a constant (near 1) for the range of

TABLE 2. Mean product of fraction of abrader impacting aggregates (F_{ani}) and aggregate abrasion coefficients (C_{ani}) for various mixtures of aggregates. No significant difference between treatments (0.10 level)

Treatment			Mean F _{ani} C _{ani} (1/m)
Mass Fraction of Large Aggregates (%)	Freestream Windspeed (m/s)	Reps	
12	12.5	3	0.023
12	15.5	2	0.023
33	12.5	9	0.015
33	15.5	5	0.019
60	13.1	2	0.024
60	12.8	2	0.021
67	15.5	5	0.015

test conditions. Note that the C_{ani} for the crusts tested in experiment 1 had about 10 times the C_{ani} of the aggregates in this test. This is the reason it is necessary to distinguish between aggregates and crusts when computing soil loss by abrasion.

Additional low speed tests are needed to determine the conditions at which F_{ani} decreases. As wind speed decreases, there are two reasons for F_{ani} to decrease. First, the rate of emission of saltation-size aggregates is proportional to the difference between saltation transport capacity and actual q. Thus, at low wind speeds, the exposed saltation-size aggregates remain on the surface longer. Second, the surface shearing stress is decreased so that portions of the surface can be sheltered from significant emission but still have saltation impacts.

On large fields, the saltation transport capacity can be reached, but abrasion will continue to break down the exposed clods and crust. As a result, the downwind portions of eroding fields often have abundant amounts of loose soil (low F_{ani}), which in extreme cases may start to form small dunes.

SUMMARY AND CONCLUSIONS

The wind erosion process on agricultural soils is being modeled as the time-dependent conservation of mass transport of soil moving as saltation and creep. Emission and abrasion act as sources, whereas trapping and suspension act as sinks for the moving soil. In this study, an expression (equation 13) for the vertical abrasion flux (G_{an}) was derived as

$$G_{an} = \left(\sum_{i=1}^n F_{ani} C_{ani} \right) q \quad (20)$$

Prior chamber studies on individual aggregates demonstrated that abrasion losses by impacting saltation-size particles were proportional to the kinetic energy of the impacting abrader. In this study, an approximate, theoretical analysis showed that impact kinetic energy per unit area imparted to a field surface should depend on the total saltation discharge (q) but be nearly independent of wind speed and ratio of q to transport capacity. To test the theory, abrasion loss rates from crusted trays were measured in the wind tunnel. A range of wind speeds and upwind sand saltation discharge rates were used to create a wide range of saltation trajectories, as confirmed by sampling vertical profiles of the saltation discharge. Abrasion loss rates from target crusts were shown to be proportional to the product of an abrasion coefficient, C_{an}, and q. Further, in agreement with theory, the value of C_{an} depended mainly on dry stabilities of the target soils and not on mean abrader trajectories.

A second series of crusted trays covered with various fractions of nonabradable aggregates were also abraded by saltating sand in the wind tunnel. These measurements confirmed that the fraction of abrader impacting surface aggregates (F_{ani}) (as opposed to crust or loose material) could be predicted directly from values for aggregate cover and surface roughness, where the latter was represented as a Weibull distribution of the shelter angles.

Finally, a third series of trays filled with various mixtures of large aggregates and saltation-size aggregates were abraded in the wind tunnel by a low saltation discharge from a narrow upwind bed. The results showed that, when saltation transport capacity significantly exceeds the actual saltation discharge, the surface tends to armor with large aggregates, and thus, F_{ani} remains near 1 for a wide range of aggregate mixtures.

REFERENCES

- Anderson, R.S. and B. Hallet. 1986. Sediment transport by wind: Toward a general model. *Geol. Soc. Am. Bull.* 97:523-535.
- Chepil, W.S. and N.P. Woodruff. 1963. The physics of wind erosion and its control. *Adv. in Agron.* 15:211-302.
- Hagen, L.J. 1984. Soil aggregate abrasion by impacting sand and soil particles. *Transactions of the ASAE* 27(3):805-808, 816.
- . 1988. Wind erosion prediction system: an overview. ASAE Paper No. 88-2554. St. Joseph, MI: ASAE.
- . 1990. A wind erosion prediction system to meet user needs. *J. Soil and Water Conserv.* 46(2):106-111.
- Hagen, L.J. and L. Lyles. 1985. Amount and nutrient content of particles produced by soil aggregate abrasion. In: *Proc. of the National Symposium on Erosion and Soil Productivity* 8-(85):117-129.
- Hagen, L.J., E.L. Skidmore and J.B. Layton. 1988. Wind erosion abrasion: effects of aggregate moisture. *Transactions of the ASAE* 31(3):725-728.
- Potter, K.N., T.M. Zobeck, and L.J. Hagen. 1990. A microrelief index to estimate soil erodibility by wind. *Transactions of the ASAE* 33(1):151-155.
- Skidmore, E.L. and D.H. Powers. 1982. Dry soil-aggregate stability: Energy-based index. *Soil Sci. Soc. Am. J.* 46:1274-1279.
- Sorensen, M. 1985. Estimation of some aeolian saltation transport parameters from transport rate profiles. In *Proc. Int. Workshop on Physics of Blown Sands*, Univ. of Aarhus, Denmark 1(8):141-190.
- White, B.R. 1982. Two-phase measurements of saltating turbulent boundary layer flow. *Multiphase Flow* 8(5):459-473.
- Willets, B.B. and M.A. Rice. 1985. Inter-saltation collisions. In *Proc. Int. Workshop on Physics of Blown Sands*, Univ. of Aarhus, Denmark 1(8):83-100.
- Woodruff, N.P. and F.H. Siddoway. 1965. A wind erosion equation. *Soil Sci. Soc. Am. Proc.* 29:602-608.

SYMBOLS

(M, L, and T as dimensions refer to mass, length, and time)

Symbol	Definition and dimensions
\bar{C}	Average concentration of particles within the control volume, ML^{-3}
C_1	Coefficient, T^2L^{-2}
C_{an}	Coefficient of abrasion, L^{-1}
E_o	Loose soil removable by wind alone, ML^{-2}
EU, EV	Components of horizontal windspeed in X and Y directions, respectively, LT^{-1}

F_{ani}	Fraction of impacting saltation striking the ith surface cover
F_c	Mass fraction of aggregates larger than saltation-size
F_{sc}	Fraction of surface cover of aggregates larger than saltation size
$F(S_a)$	Cumulative fraction of shelter angles less than angle S_a
g	Acceleration of gravity, LT^{-2}
G_i	Vertical flux of impacting particles following ith trajectory, $ML^{-2}T$
G_{an}	Net vertical flux from abrasion of aggregates and crust, $ML^{-2}T^{-1}$
G_{en}	Net vertical flux from emission of loose soil, $ML^{-2}T^{-1}$
G_{enz}	Net vertical flux from emission of loose soil initially protected by large aggregates, $ML^{-2}T^{-1}$
G_{ss}	Net vertical flux of suspension-size soil particles, $ML^{-2}T^{-1}$
G_{tp}	Net vertical flux from trapping saltation-size particles, $ML^{-2}T^{-1}$
H	Distance from soil surface to top of control volume, L
K_p	Dimensionless coefficient
L_i	Average particle jump length of particles on ith trajectory, L
q	Horizontal saltation discharge, $ML^{-1}T^{-1}$
q_i	Horizontal saltation discharge of particles on ith trajectory, $ML^{-1}T^{-1}$
q_{max}	Maximum horizontal saltation discharge for a given windspeed (transport capacity) $ML^{-1}T^{-1}$
q_x, q_y	Components of the saltation discharge in x and y directions, respectively, $ML^{-1}T^{-1}$
RR1	Scale factor of Weibull shelter angle distribution, degrees
RR2	Shape factor of Weibull shelter angle distribution
S_a	Shelter angle, degrees
t	Time, T
TL	Total soil loss, ML^{-2}
U_*	Surface friction velocity, LT^{-1}
u_i	Horizontal component of abrader impact velocity of particles on ith trajectory, LT^{-1}
V_{an}	Volume of soil abraded from large aggregates, L^3L^{-2}
V_{en}	Volume of loose soil emitted which was initially protected by large aggregates, L^3L^{-2}
V_i	Impact velocity of particles on ith trajectory, LT^{-1}
\bar{V}_p	Average horizontal saltating particle velocity, LT^{-1}
w_i	Vertical component of abrader impact velocity, LT^{-1}
WU	Horizontal wind speed, LT^{-1}
x, y	Horizontal distances in perpendicular directions parallel to rectangular field boundaries, L
z_i	Maximum jump height of particles on ith trajectory, L
θ_i	Average abrader impact angle relative to the surface for particles on the ith trajectory, degrees